# Ising model of polarity formation in molecular crystals:
# From the growth model to the asymptotic equilibrium state

H. Bebie,[1,*] J. Hulliger,[2] S. Eugster,[1] and M. Alaga-Bogdanović[2]

[1]*Institute for Theoretical Physics, University of Berne, CH-3012 Berne, Switzerland*
[2]*Department of Chemistry and Biochemistry, University of Berne, CH-3012 Berne, Switzerland*
(Received 21 December 2001; published 28 August 2002)

We analyze a layer-by-layer growth model of crystals consisting of dipolar molecules with two directional states. The model is characterized by the assumption of thermal equilibrium formation of new adlayers, whereas previous layers are treated as being "frozen" in the state in which they were formed. Longitudinal and transverse Ising-type nearest neighbor interactions are taken into account. Under such assumptions, bulk polarization is known to arise. We mainly consider asymptotic one- and two-layer statistics after many steps of growth; we have obtained a theorem relating this statistics to thermal equilibrium of an appropriate two-layer system. Local polarization patterns resembling those of ferromagnetism and antiferromagnetism emerge, depening on signs and magnitudes of the coupling constants. We have explored such effects by means of simulations, by a mean field approximation, and by a Bethe-Peierls analysis.

## I. INTRODUCTION

Recently, we have shown that a macroscopic state featuring polar properties may arise as a result of orientational selectivity of dipolar molecules being attached to a crystal surface during growth [1]. In view of different growth speeds, we have to distinguish between effects being kinetic in nature and those related to conditions of thermal equilibrium. In the present work we consider phenomena in the limit of slow growth, where it is reasonable to assume that adlayers are formed in thermal equilibrium. Scanning pyroelectric microscopy, phase-sensitive second-harmonic microscopy [2,3], and Markov-chain [4,5] studies providing examples and understanding of spontaneously evolving polar properties during the growth of host-guest and single-component molecular crystals have introduced a fundamentally new view on how molecular crystals built from dipolar molecules can develop a pyroelectric symmetry class by a mechanism of growth. As shown previously [6], the Markov-chain mechanism of polarity formation can transform a centrosymmetric seed crystal, e.g., $P2_1/c$, into a twinned state, where polar properties develop in the positive and negative $b$ sector. As shown by phase-sensitive second-harmonic microscopy [7], the direction of the net polarization in these sectors is opposite.

The system to be investigated here is defined as follows: A single-component crystal built up from dipolar molecules is subjected to slow layer-by-layer growth. Dipolar entities [represented by donor ($D$) and acceptor ($A$) type molecular fragments bound to a $\pi$-conjugated frame] are attached to a face ($hkl$) of whatever the given seed crystal structure is. Among the possible processes which can occur during the attachment of molecules to surface sites, we consider only those with one degree of freedom: the up or down orientation of the dipole moment of the admolecules. For the ($hkl$)-substrate layer itself (i.e., the layer attached in the previous step), no degree of freedom with respect to up or down is allowed. For the molecular crystals we are considering here, the assumption of a frozen substrate is justified due to the very large energy of activation for a reversal of the polar orientation of molecules within the substrate layer ($E_a > 50$ kJ/mol for prolate top molecules). Arranged as this, we investigate the evolution of orientational order, especially for long sequences of layer-by-layer growth. Independent of whether growth started from a perfectly ordered centrosymmetric or noncentrosymmetric substrate seed crystal, each adlayer will accomodate some degree of orientational ordering, the statistics being determined by the requirement of the global minimum of the free energy of an adlayer. The present concept is fresh and has not been considered by the standard models of crystal growth of molecular materials. Application is widespread, because all crystals built from dipolar molecules, at least in principle, are expected to show grown-in effects of polarity. Typical candidates are derivatives of benzene- and stilbene-type frameworks. For examples, see [5].

In the present work we will address the interesting question as to whether the limiting layer statistics—after an arbitrarily large number of growth steps—can be conceived in some sense as a thermal equilibrium statistics of an isolated system. In fact, we have found that the asymptotic statistics of the two-layer system consisting of the thermalized adlayer and the previously formed substrate is the canonical distribution of a two-layer system with appropriate interactions. This allows us to set up an Ising-type Hamiltonian to discuss phase transitions as a function of coupling parameters and temperature. In the sections to follow we have worked out a formalism describing this equivalence. Monte Carlo methods are used to portray the basic behavior of the system during growth. Average values of layer polarization and phase transition characteristics are calculated by a mean field as well as by a Bethe-Peierls approximation.

Some of our assumptions are very close to those formulated in a model for growth of binary alloys [8], where atoms are allowed to interact and to equilibrate at the surface, but are frozen in the bulk. In that model too, the asymptotic layer

_____
*Electronic address: bebie@itp.unibe.ch
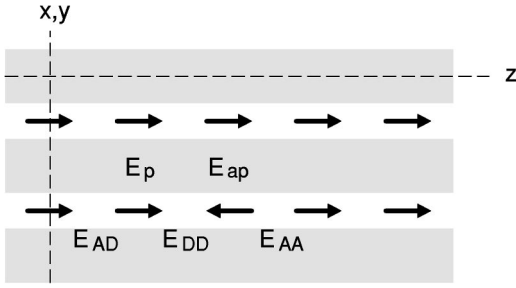
FIG. 1. Interactions between dipolar molecules (arrows). The arrows indicate the orientational state of the dipolar molecules ($A \rightarrow D$ or $D \leftarrow A$; polarizations $+1$ and $-1$ with respect to the direction of growth). $z$: direction of growth. $x$, $y$ : transverse directions (2D). $E_{AD}$, $E_{DD}$, $E_{AA}$ : nearest neighbor longitudinal interaction energies. $E_p$, $E_{ap}$ : nearest neighbor transverse interaction energies. Layer-by-layer growth gives rise to net bulk polarization.

statistics (beyond a transient thickness) was proved to correspond to the thermal equilibrium of a two-layer system. In our case, however, the corresponding theorem is more complicated, due to the fact that the longitudinal interaction has less symmetry in our case. Details are worked out in Sec. V.

## II. GROWTH MODEL: DEFINITION OF INTERACTIONS

In the model discussed in the present paper, a rectangular crystal is growing layer-by-layer in the positive $z$ direction. Molecules are arranged on a square lattice. The number of molecules per layer is denoted by $N = n_x n_y$ (usually, $n_x = n_y$). The molecules are of the dipolar type featuring simply two directional states ($s = \pm 1$ in the $z$ direction). Nearest neighbor interactions among dipolar molecules within the same layer and between adjacent layers are assumed, the pair interaction energy depending on the directional states of the two molecules involved. The main assumptions on the layer-by-layer growth process are the following: (i) A new layer starts to be formed only after the preceding layer is completed. (ii) When a new layer is attached, the former layers (indices $0, \ldots, z$) are assumed to be "frozen" (i.e., they are kept fixed permanently in the state in which they were formed), whereas the new layer (index: $z+1$) relaxes to thermal equilibrium, taking the nearest neighbor interactions of dipolar molecules within the layer and with corresponding sites of the formerly grown layer into account. (iii) Thermal relaxation of a layer takes place after all its molecules are attached. (iv) The state of the seed layer ($z = 0$) is given explicitly. These assumptions are supported by the fact that in molecular crystals of elongated prolate-type molecules, the activation energy for dipole reversal in the substrate layer is high and that molecular crystals generally do not undergo surface reconstruction. Thermal relaxation of the surface layer will not always be met: this assumption requires the surface layer to have sufficient time to equilibrate, before it is completed, i.e., the time for the growth of a layer must be larger than surface layer relaxation times. This issue is discussed in Ref. [8] in connection with growth of binary alloys. More precisely, we assume the following interactions among dipolar molecules (see Fig. 1).

TABLE I. Longitudinal interactions between molecules of adjacent layers at corresponding sites.

| Layer $z$ $s'$ | Layer $z+1$ $s$ | Energy | $R(s',s)$ |
|---|---|---|---|
| $-$ | $-$ | $E_{AD}$ | 0 |
| $-$ | $+$ | $E_{AA}$ | $A = \Delta E_A / kT$ |
| $+$ | $-$ | $E_{DD}$ | $D = \Delta E_D / kT$ |
| $+$ | $+$ | $E_{AD}$ | 0 |

(a) *Transverse interactions*. We assume nearest neighbor Ising interactions between dipolar molecules within the same layer. $\Delta E_\perp = E_p - E_{ap}$ denotes the pair energy difference between parallel and antiparallel polarizations. We introduce the dimensionless coupling $Q_\perp = \Delta E_\perp / kT$. A negative value of $Q_\perp$ favors equal polarization of neighbors within layers.

(b) *Longitudinal interactions*. The polarization vector of a dipolar molecule points from the electronic acceptor terminal ($A$) to the electronic donor ($D$) terminal, symbolically $A \rightarrow D$. In Table I, $s'$ denotes the polarization of the molecule of layer $z$ (formerly grown, now frozen), $s$ the polarization of the molecule of layer $z+1$ (being attached and thermalized), both at the same site ($x, y$). $E_{AA}$ stands for the interaction energy between $A$ and $A$ terminals ($s' = -1$, $s = +1$; $DA \cdots AD$), likewise $E_{DD}$ for $AD \cdots DA$ and $E_{AD}$ for $AD \cdots AD$ or $DA \cdots DA$. Without loss of generality, interaction energies can be given with respect to $E_{AD}$; basic parameters, therefore, are $\Delta E_A = E_{AA} - E_{AD}$ and $\Delta E_D = E_{DD} - E_{AD}$. The dimensionless couplings $R$ are expressed in terms of $A = \Delta E_A / kT$ and $D = \Delta E_D / kT$ (see Table I). Intermolecular interaction energies are accessible by quantum mechanics calculations [9,10]. Typical values for $E_{AA}$, $E_{DD}$, $E_{AD}$ range from several to about 40 kJ/mol. Examples are the known H-bond-type interactions. The majority of the examples given in Ref. [5] belong to the sector $\Delta E_A$, $\Delta E_D$, $\Delta E_\perp > 0$; in these cases, the coupling is ferromagnetic in the direction of growth, and antiferromagnetic perpendicular to it (Fig. 2, row d). For a systematic account of possible phenomena we shall also treat other sectors of the coupling constants.

To summarize, one step of the growth process consists of the attachment of a complete new layer in thermal equilibrium under the influence of its internal transverse interactions and of the interactions with the former layer. The two-dimensional (2D) Ising-type Hamiltonian $H_1$ determining thermal equilibrium of the new layer (with polarizations $s_{xy}$, $x = 1, \ldots, n_x$, $y = 1, \ldots, n_y$) under the influence of the fixed state of the former layer (described by its polarizations $s'_{xy}$) is

$$H_1(\{s\})/kT = \sum_{x,y} \frac{Q_\perp}{2} s_{x,y}(s_{x,y+1} + s_{x+1,y})$$

$$+ \sum_{x,y} R(s'_{x,y}, s_{x,y}), \quad (1)$$

where $R(s', s)$ is defined in Table I. For the transverse interactions boundary conditions have to be formulated, usually
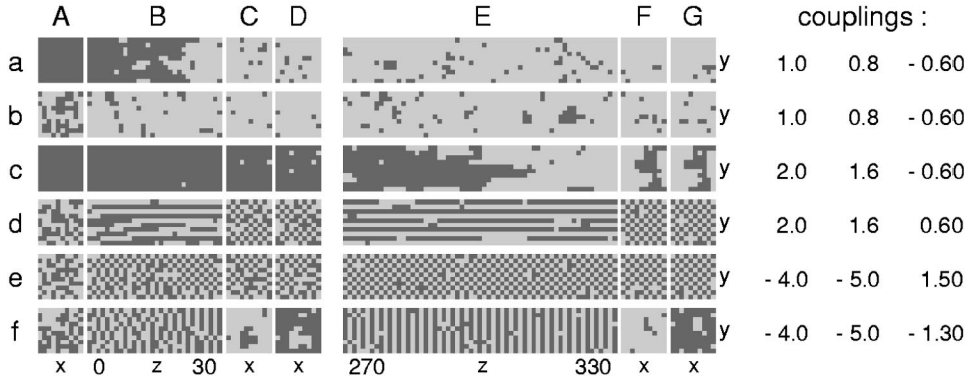
FIG. 2. Simulation of typical growth processes. Layer size $10 \times 10$. $x$, $y$, $z$ denote the axes ($z$: direction of growth, from left to right). Squares display single layers, rectangles show side views (plane $x=0$). Columns: (A) layer $z=0$ (seed, given explicitly), (B) side view ($z=0$–$30$), (C) layer $z=29$, (D) layer $z=30$, (E) side view ($z=270$–$330$), (F) layer $z=329$, (G) layer $z=330$. Last three columns: couplings ($A$, $D$, $Q_\perp$). Rows: (a) uniformly polarized seed ($s_0 = +1$), (b) randomly polarized seed, (c) initial configuration metastable, switching to a stable one at about $z=300$, (d) layer organization AFO, (e) polarizations alternating from layer to layer, layer organization AFO, (f) polarizations alternating from layer to layer, layer organization FO.

either open or periodic, and taken care of in the first sum of Eq. (1). In simulations we use periodic boundary conditions.

## III. BASIC PHENOMENA IN ($A$, $D$, $Q_\perp$) SPACE

The thermal character of the formation of new layers calls for a statistical description of the crystal. Given the layer size $n_x$, $n_y$, the process is fully determined by the couplings $A$, $D$, $Q_\perp$ and by the state of the initial layer ($z=0$). It does not come as a surprise that the memory for the initial state gets lost in the course of the growth process. In the present paper we are mainly concerned with the asymptotic statistics of the layer after many steps and for the asymptotic correlation between a layer and its predecessor (in the present paper quoted as the large-$z$ limit).

The main characteristics of the growth process for any given set of couplings and for different initial conditions can be observed by means of simulations. Some examples are displayed in Fig. 2. Typical layers remind of Ising-like structures, due to the influence of the transverse interaction. For negative values of $Q_\perp$, ferromagnetic ordering (FO) with a tendency to equal polarization of neighbors can be expected, whereas positive values of $Q_\perp$ favor local antiferromagnetic ordering (AFO) within the same layer. In longitudinal direction two main patterns can be observed, again depending on the couplings: either the new layer reproduces more or less the previous one, or its polarities are opposite to the previous ones at corresponding sites.

In full generality, the asymptotic statistics (large-$z$ limit) ought to be described for all points of the parameter space ($A,D,Q_\perp$). For the sake of an overview, the remainder of the present section is restricted to a discussion of the following special cases: (i) $Q_\perp \to \infty$, (ii) $Q_\perp \to -\infty$, (iii) no transverse coupling, $Q_\perp = 0$, (iv) dependence on $Q_\perp$ for some fixed $A > 0$, $D > 0$ (always in the large-$z$ limit).

(i) For $Q_\perp \to \infty$, the layer exhibits a checkerboardlike pattern (AFO): $s_{xy} = s_0(-1)^{x+y}$, where the signature $s_0$ is $+1$ or $-1$. The energy required to change the signature from one layer to the next is $N(\Delta E_A + \Delta E_D)/2$. Therefore, for finite

layer size $N$, the probability $p_c$ of the signature to change from one layer to the next is given by

$$p_c = \frac{1}{1 + e^{N(A+D)/2}}. \quad (2)$$

For large $N$ and fixed $A$ and $D$, this formula gives a simple picture for the transition from one layer to the next: for $A + D < 0$ the signature will alternate; for $A + D > 0$, the signature remains the same (see Fig. 3, right). The examples displayed in Fig. 2 [rows (d) and (e)] approximate this behavior. The switching behavior is already discussed in [5,11].

(ii) For $Q_\perp \to -\infty$, the layer is homogeneous (FO): $s_{xy} = s_0$, where the layer polarization $s_0$ is $+1$ or $-1$. The transition probabilities $p_{s_0' s_0''}$ from layer polarization $s_0'$ to $s_0''$ are given by

$$p_{++} = (1 + e^{-ND})^{-1}, \quad p_{+-} = (1 + e^{ND})^{-1},$$

$$p_{-+} = (1 + e^{NA})^{-1}, \quad p_{--} = (1 + e^{-NA})^{-1}. \quad (3)$$
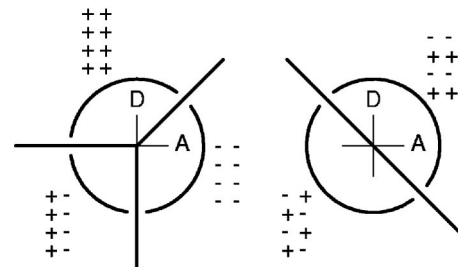


FIG. 3. Idealized layer statistics and layer pair statistics for large transverse interaction in the large-$z$ limit. Left: $Q_\perp \to -\infty$. Right: $Q_\perp \to +\infty$. Symbols $+$ and $-$ indicate local polarizations (four sites of two consecutive layers). Layer organization may be of FO or AFO type, and may reproduce or alternate from one layer to the next. For each of the five different regimes an example can be found in Fig. 2.

TABLE II. Attachment of an admolecule: summary of eight situations (mean field approximation). $s'$, polarization of substrate molecule; $s$, polarization of admolecule at same site. The mean field estimate of the coupling energy depends on the sublattice $g$ to which the site belongs.

| | Sublattice $g$ | $s'$ | $s$ | Coupling | Branching probability |
|---|---|---|---|---|---|
| 1 | 2 | − | − | $+2Q_\perp(1-2q^{(1)})$ | $v_1$ |
| 2 | 2 | − | + | $-2Q_\perp(1-2q^{(1)})+A$ | $v_2=1-v_1$ |
| 3 | 2 | + | + | $-2Q_\perp(1-2q^{(1)})$ | $v_3$ |
| 4 | 2 | + | − | $+2Q_\perp(1-2q^{(1)})+D$ | $v_4=1-v_3$ |
| 5 | 1 | − | − | $+2Q_\perp(1-2q^{(2)})$ | $v_5$ |
| 6 | 1 | − | + | $-2Q_\perp(1-2q^{(2)})+A$ | $v_6=1-v_5$ |
| 7 | 1 | + | + | $-2Q_\perp(1-2q^{(2)})$ | $v_7$ |
| 8 | 1 | + | − | $+2Q_\perp(1-2q^{(2)})+D$ | $v_8=1-v_7$ |

From this matrix we obtain the mean lengths $\bar{L}_\pm$ of chains of equally polarized layers (polarities $+1$ or $-1$, repectively),

$$\bar{L}_+=1+e^{ND}, \qquad \bar{L}_-=1+e^{NA}. \qquad (4)$$

In the large-$N$ limit these expressions imply the following picture of the transition behavior. For the sector $A<0, D<0$ the polarization alternates from layer to layer. For $D>0$, $D>A$, starting from any state of the first layer ($z=0$) the asymptotic layer polarization is 1 ($z\to\infty$); for $A>0$, $A>D$, the asymptotic layer polarization is $-1$ (see Fig. 3, left). In the sector $A>0, D>0$ there are metastable states, such as, for example, the layer state $s_0=-1$ in the range $D>A>0$, due to the extremely small transition probability $\approx e^{-NA}$ from layer polarization $-1$ to $+1$; similarly, $s_0=+1$ is metastable in the range $A>D>0$.

(iii) We now consider the case of missing transverse coupling, $Q_\perp=0$, which is well known from the 1D treatment of the present model ($n_x=n_y=1$) [4]. Along the direction of growth, a site $(x,y)$ undergoes a stochastic process with fixed transition probabilites from one polarization to the other, the mean length of chains of constant polarization being given by

$$\bar{L}_{1+}=1+e^{D}, \qquad \bar{L}_{1-}=1+e^{A}. \qquad (5)$$

More details on the single chain can be found in the Appendix.

(iv) Finally, we assume $A>0$ and $D>0$ to be held fixed and discuss the behavior of the layer as a function of $Q_\perp$. The most prominent feature is the phase transition to the AFO state occurring at some value $Q_\perp=Q_\perp^{(\text{crit})}(A,D)>0$, such that for $Q_\perp>Q_\perp^{(\text{crit})}$ the two sublattices have a different mean polarization (sublattice 1, $x+y=$ odd; sublattice 2, $x+y=$ even); for $Q_\perp<Q_\perp^{(\text{crit})}$ the layer is homogeneous. The behavior at $Q_\perp=Q_\perp^{(\text{crit})}$ (for fixed $A,D$) corresponds to the ferromagnetic-antiferromagnetic transition in magnetism in the presence of an external field. More details on this phenomenon will be given in Secs. IV and VI.

## IV. MEAN FIELD DESCRIPTION

In the present section we restrict ourselves to the sector $A>0$, $D>0$ and use a mean field approximation to discuss the stationary layer statistics (large-$z$ limit), which is expected to exist in this sector. This approximation turns out to be sufficient for an understanding of the AFO-phase transition (see below).

For sufficiently large positive values of $Q_\perp$ the layer is expected to exhibit approximately an AFO structure (see Sec. III), i.e., markedly different spatial averages of the polarization for the two sublattices. In view of this effect we introduce separate spatial mean polarizations $s^{(1)}$ and $s^{(2)}$ for the two sublattices $g$ ($g=1,2$). The probability of a site of sublattice $g$ to have positive polarization is $q^{(g)}=(s^{(g)}+1)/2$. In the spirit of the mean field approximation we disregard local correlations. In view of the symmetry between the two sublattices, we may introduce the convention $q^{(2)}\leq q^{(1)}$.

Let us consider a site $(x,y)$ of the substrate layer (polarization $s'$); $s$ denotes the polarization of the molecule to be attached at the corresponding site $(x,y)$ of the new layer. The eight possible situations are listed in Table II. The column "coupling" gives the expectation value of the coupling energies (divided by $kT$). Given the state $s'$ of the substrate molecule and its sublattice, there is a pair of two competing processes, $s'\to-1$ or $s'\to+1$ (such as, for example, processes 1 and 2). Note that the mean field estimate of the couplings assumes thermalization of the adlayer after all its molecules are attached.

Based on the assumption of the thermal equilibrium formation of the new layer, the probabilities $v_i$ defined in Table II are given by the following expressions (derived from the mean field estimate of the energy difference within the pair, see Table II):

$$v_1=[1+e^{+4Q(1-2q^{(1)})-A}]^{-1}, \qquad (6)$$

$$v_3=[1+e^{-4Q(1-2q^{(1)})-D}]^{-1}, \qquad (7)$$

$$v_5=[1+e^{+4Q(1-2q^{(2)})-A}]^{-1}, \qquad (8)$$

$$v_7=[1+e^{-4Q(1-2q^{(2)})-D}]^{-1}. \qquad (9)$$
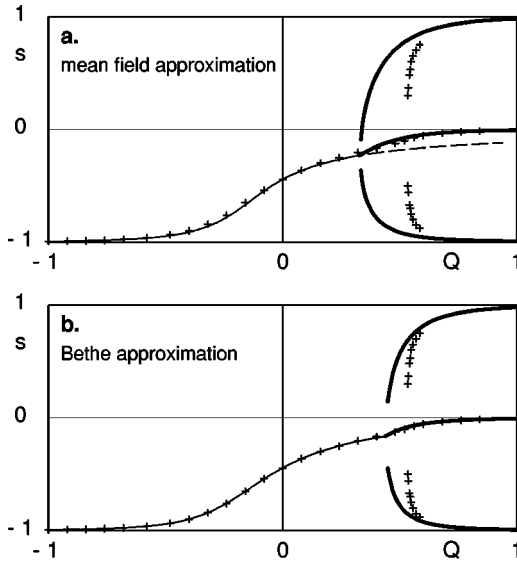
FIG. 4. Layer polarization in the large-$z$ limit. $A = 2.0$, $D = 0.8$. Abscissa: $Q_\perp$. Ordinate: sublattice and mean layer polarization. (a) Mean field approximation, (b) Bethe approximation. Thin line, FO type solution ($s^{(1)} = s^{(2)}$); solid thin line, physical FO range; broken thin line, unphysical range of FO -type solution. Thick lines: sublattice and mean polarizations in AFO range. + : simulation results.

For the asymptotic statistics ($z \to \infty$), the probabilities $q^{(s)}$ are the same for both layers, leading to the following equations of consistency:

$$q^{(1)}(1 - v_7) = (1 - q^{(1)})(1 - v_5), \tag{10}$$

$$q^{(2)}(1 - v_3) = (1 - q^{(2)})(1 - v_1). \tag{11}$$

After inserting $v_1, \ldots, v_7$ from Eqs. (6)–(9), this pair of equations determines $q^{(1)}$ and $q^{(2)}$ for given $A$, $D$, $Q_\perp$. First we extract the solutions with the property $q^{(1)} = q^{(2)} = q$, corresponding to equal sublattice polarizations. These FO type solutions are expected to exist at least for negative values of $Q_\perp$. In this case Eq. (11) or Eq. (10) can easily be solved for $Q_\perp$,

$$Q_\perp(q) = \frac{1}{4(1 - 2q)}$$

$$\times \ln \left[ \frac{(2q - 1) + \sqrt{(2q - 1)^2 + 4q(1 - q)e^A e^D}}{2e^D(1 - q)} \right]. \tag{12}$$

The curve in the $(Q_\perp, q)$ plane obtained from this relation may be termed the FO curve in mean field approximation [Fig. 4(a), thin line]. Note that for $A > D > 0$ the branch $0 < q < 0.5$ has to be taken, and for $D > A > 0$ the branch $0.5 < q < 1$. As we shall see below, the solution (12) is unphysical beyond some positive value of $Q_\perp$, where the transition to the AFO state occurs ($A > 0$ and $D > 0$ held fixed and $Q_\perp$ increasing).

We now turn our attention to solutions of the type $q^{(1)} \neq q^{(2)}$, corresponding to different sublattice polarizations

(AFO -type solution). They can be found numerically from the pair of equations (10), (11). It turns out that they do exist for given $A > 0$, $D > 0$ for values of $Q_\perp$ exceeding some positive critical value $Q_\perp^{(\text{crit})}(A, D)$. Intuitively it is clear that these solutions correspond to the expected AFO behavior of layers for sufficiently large positive values of $Q_\perp$. Figure 4(a) displays the sublattice polarizations $s^{(1)}$, $s^{(2)}$ and the mean layer polarization $s = (s^{(1)} + s^{(2)})/2$ as functions of $Q_\perp$ (thick lines). In this range, $Q_\perp^{(\text{crit})} < Q_\perp$, the solutions of the type $q^{(1)} = q^{(2)}$ found previously must be unstable: they are artifacts of our system of equations [Fig. 4(a), dashed line].

At the phase transition the mean field approximation for $s(Q_\perp)$ exhibts a kink [Fig. 4(a)]. The kink is also obtained in the Bethe approximation [see Sec. VI and Fig. 4(b)]. So far we could not reproduce this kink in our simulations (Fig. 4, symbols +). Simulation results for layer sized $50 \times 50$ and $100 \times 100$ were obtained by means of the method developed in Sec. VI (canonical distribution of an equivalent two-layer system). Typically, $10^{10}$ Monte Carlo trials were carried out for a given set of parameters ($A$, $D$, $Q_\perp$). Sublattice polarizations in the AFO range were estimated from the peaks of their distribution. In our programs we used the random number generator introduced by Bays and Durham as described in Ref. [12].

The critical value $Q_\perp^{(\text{crit})}$ depends only weakly on $A$ and $D$. For $A = D = 0$ we obtain $Q_\perp^{(\text{crit})} = 1/2$, the well known critical value in the mean field approximation of the Ising model. For $A = 2$ and $D = 0.8$ the mean field approximation yields $Q_\perp^{(\text{crit})} \approx 0.33$ (0.54 from simulations).

Though the mean field description (MFD) presented in this section is not expected to match the behavior of our process accurately, it has some remarkable merits.

(i) For typical values of $A$ and $D$ and for any $Q_\perp$, the MFD polarization agrees reasonably well with simulation results;

(ii) The MFD is able to account for the existence of an AFO phase transition, where the polarizations of the two sublattices assume different values spontaneously (with a critical exponent of 1/2); it is observed, e.g., at fixed $A$, $D$ with increasing $Q_\perp$.

(iii) For $Q_\perp = 0$, the chains are independent and the exact mean polarization can be taken from the isolated chain analysis (see Appendix),

$$s(Q_\perp = 0) = \frac{e^D - e^A}{2 + e^D + e^A}. \tag{13}$$

The same result follows from the MFD [Eq. (12), $Q_\perp = 0$].

(iv) At $Q_\perp = 0$, even the slope $ds/dQ_\perp$ as given by the MFD is exact,

$$\left. \frac{ds}{dQ_\perp} \right|_{Q_\perp = 0} = 8 \frac{e^{2A}(1 + 2e^D) - e^{2D}(1 + 2e^A)}{(2 + e^A + e^D)^3}. \tag{14}$$

This expression can be derived by differentiating Eq. (11) or Eq. (10) with respect to $Q_\perp$, setting $Q_\perp = 0$, solving for $dq/dQ_\perp$, and finally $ds/dQ_\perp = 2dq/dQ_\perp$. Remember that we have $q^{(1)} = q^{(2)} = q$ at $Q_\perp = 0$. The exactness of Eq. (14)

is due to the following properties of the MFD: (i) the result for $s$ is exact at $Q_\perp = 0$, and (ii) the influence of the transverse coupling on the transition probabilities is taken into account exactly up to first order in $Q_\perp$ (first-order perturbation obtained from the expectation value of the transverse coupling in the unperturbed state).

## V. THE ASYMPTOTIC DISTRIBUTION OF THE LAYER STATE ($z \to \infty$)

In this section we concern ourselves with the asymptotic distribution $\pi_\sigma$ of the states $\sigma$ ($\sigma = 1, \ldots, 2^N$) of the front layer after infinitely many steps (layer index $z \to \infty$). A state $\sigma$ of a layer is specified by the values of all polarizations, $\{s_{xy}\}$. All statistics of the growth process, including the asymptotic distribution, is determined by the transition matrix $P$: its elements $P_{\sigma'\sigma}$ are the transition probabilities from a given (frozen) substrate layer state $\sigma'$ to the state $\sigma$ of the newly attached layer. From the assumptions of the growth model, we have

$$P_{\sigma'\sigma} = \frac{\Lambda_{\sigma'\sigma}\Gamma_\sigma}{\sum_{\sigma''} \Lambda_{\sigma'\sigma''}\Gamma_{\sigma''}}, \tag{15}$$

where

$$\Lambda_{\sigma'\sigma} = \exp(-E^{\text{long}}_{\sigma'\sigma}/kT), \tag{16}$$

$$\Gamma_\sigma = \exp(-E^{\text{trans}}_\sigma/kT). \tag{17}$$

$E^{\text{long}}_{\sigma'\sigma}$ denotes the longitudinal coupling energy between the substrate layer state $\sigma'$ and the state $\sigma$ of the attached layer, and $E^{\text{trans}}_\sigma$ is the total energy originating from the transverse couplings within the layer state $\sigma$.

The asymptotic distribution $\pi$ must satisfy

$$\sum_{\sigma'} \pi_{\sigma'} P_{\sigma'\sigma} = \pi_\sigma, \tag{18}$$

$$\sum_\sigma \pi_\sigma = 1. \tag{19}$$

We claim that the vector $\pi$ with elements

$$\pi_\sigma = c\, e^{N^+_\sigma D + N^-_\sigma A}\Gamma_\sigma \sum_{\sigma''} \Lambda_{\sigma\sigma''}\Gamma_{\sigma''} \tag{20}$$

provides the solution of Eq. (18) [13]; $c$ denotes the normalization factor to be adjusted to satisfy Eq. (19); $N^s_\sigma$ is the number of molecules of polarization $s$ in the state $\sigma$ of the layer. This theorem can be verified by inserting expressions (15) and (20) into both sides of Eq. (18). After cancellation of sums of the type $\Sigma_{\sigma''}\Lambda_{\sigma'\sigma''}\Gamma_{\sigma''}$ on the left, the two sides are seen to be identical, if the equality

$$e^{N^+_\sigma D + N^-_\sigma A}\Lambda_{\sigma\sigma'} = e^{N^+_{\sigma'} D + N^-_{\sigma'} A}\Lambda_{\sigma'\sigma} \tag{21}$$

holds. Note that this equation does not involve the transverse interactions. Due to the independence of the chains, it suffices to prove it for one single chain ($\sigma' \to s'$, $\sigma \to s$), which can easily be worked out for the four combinations of $s', s$.

### A. The asymptotic distribution of layer states as a canonical distribution

Equation (20) constitutes an expression for the probability $\pi_\sigma$ of a layer state $\sigma$ in the large-$z$ limit. Note that the number of terms in the sum of Eq. (20) rises exponentially with increasing number of molecules per layer; therefore, its practical value for a direct computation of $\pi_\sigma$ is rather limited. Nevertheless, an elegant formula for $\pi$, such as Eq. (20), is most welcome. In the present section we use this formula in order to prove a close relation between the asymptotic statistics of the layer-by-layer growth model (GM) on the one hand and the thermodynamic equilibrium of a certain two-layer system (subsequently termed LL) on the other.

We define

$$K_{\sigma'\sigma} = e^{N^+_{\sigma'} D + N^-_\sigma A}\Gamma_{\sigma'}\Lambda_{\sigma'\sigma}\Gamma_\sigma \tag{22}$$

and note that the probability (20) of the state $\sigma$ can be written as

$$\pi_{\sigma'} = c\sum_\sigma K_{\sigma'\sigma}. \tag{23}$$

Note that $K$ is symmetrical, $K_{\sigma'\sigma} = K_{\sigma\sigma'}$ [see Eq. (21)]. The main point is the following: the sum

$$Z = \sum_{\sigma',\sigma} K_{\sigma'\sigma} \tag{24}$$

can be interpreted as the partition sum of a certain two-layer system LL, where $\sigma'$ and $\sigma$ denote the states of its first and second layer. The interactions governing the system can be read off from $K_{\sigma'\sigma}$, in that the factors in expression (22) can be interpreted as Boltzmann factors corresponding to certain transverse, longitudinal, and external field couplings of an appropriate two-layer system. The system LL and its interactions will be described in greater detail below. From Eqs. (23) and (24) the link between this two-layer system LL and the asymptotic statistics of the GM as given by Eq. (20) is now evident: the GM probability $\pi_{\sigma'}$ is equal to the probability of the state $\sigma'$ of one of the two layers of LL (in thermodynamic equilibrium).

The structure and the interactions of the two-layer system LL defined by its partition sum $Z$ can be read off from Eq. (22).

(i) LL consists of two layers ($L'$, $L$) of the same size as the layers in the GM. Like in GM, each grid point carries the polarity $-1$ or $+1$. The index $\sigma'$ denotes the state of $L'$, $\sigma$ the state of $L$.

(ii) Factor $\Gamma_{\sigma'}$: Boltzmann factor corresponding to transverse interaction within layer $L'$, same as in the growth model. $\Gamma_\sigma$: same, layer $L$.

(iii) Factor $\Lambda_{\sigma'\sigma}$: Boltzmann factor corresponding to longitudinal interactions between the two layers, same as in the GM. (See Table I).

TABLE III. Two-layer system LL, coupling energies divided by $kT$. See Table IV for an equivalent scheme.

| $s'$ | $s$ | Longitudinal | External field | Total |
|------|-----|--------------|----------------|-------|
| $-$ | $-$ | 0 | $-A$ | $-A$ |
| $-$ | $+$ | $A$ | $-A$ | 0 |
| $+$ | $-$ | $D$ | $-D$ | 0 |
| $+$ | $+$ | 0 | $-D$ | $-D$ |

(iv) Factor $e^{N_{\sigma'}^{+}D+N_{\sigma'}^{-}A}$: Boltzmann factor corresponding to the coupling of the molecules of layer $L'$ to an external field. The energy of a polarization $+1$ or $-1$ amounts to $-D$ or $-A$, respectively. Note that this interaction applies to one of the two layers only ($L'$).

The longitudinal interaction energies (divided by $kT$) between two corresponding molecules of $L'$, $L$ (with polarizations $s'$, $s$) are summarized in Table III.

The following reinterpretation is more elegant and discloses the symmetry between the two layers. The same net interaction as described above is obtained with an external field affecting all molecules of both layers together with an appropriate longitudinal Isinglike interaction between corresponding molecules, the transverse interactions remaining the same as before (see Table IV). The Ising coupling strength (energy of parallel configuration minus energy of antiparallel configuration divided by $kT$) is

$$Q_{\parallel} = -\frac{A+D}{2}. \tag{25}$$

The external coupling of polarization $s$ is $sB$,

$$B = -\frac{D-A}{4}. \tag{26}$$

In this most symmetric formulation, the external coupling term is responsible for the predominance of positive polarity in the sector $D>A$. Note that an exchange of the two layers does not affect the energy.

To summarize, the Hamiltonian $H_2$ of the two-layer system reads

$$H_2/kT = \sum_{x,y} \frac{Q_{\perp}}{2} s_{x,y}(s_{x,y+1}+s_{x+1,y})$$

$$+ \sum_{x,y} \frac{Q_{\perp}}{2} s'_{x,y}(s'_{x,y+1}+s'_{x+1,y}) + B\sum_{x,y}(s_{x,y}+s'_{x,y})$$

$$+ \frac{Q_{\parallel}}{2} \sum_{x,y}(1+s_{x,y}s'_{x,y}), \tag{27}$$

TABLE IV. Two-layer system LL, symmetric coupling scheme.

| $s'$ | $s$ | Longitudinal | External field | Total |
|------|-----|--------------|----------------|-------|
| $-$ | $-$ | $-(A+D)/2$ | $2(D-A)/4$ | $-A$ |
| $-$ | $+$ | 0 | 0 | 0 |
| $+$ | $-$ | 0 | 0 | 0 |
| $+$ | $+$ | $-(A+D)/2$ | $-2(D-A)/4$ | $-D$ |

where $s'_{xy}$ and $s_{xy}$ denote the polarizations at site $x,y$.

The equivalence presented here seems potentially useful for the analysis of the layer-by-layer growth model.

(i) The asymptotic statistics of the GM can be obtained from a Monte-Carlo simulation of the thermal equilibrium of the system LL. All known techniques of simulating a canonical ensemble can be applied directly.

(ii) Any phase transitions suspected in simulations and approximate analyzes of GM must correspond to a thermal equilibrium phase transition in LL. Thus, phase transitions of GM get a well defined background in terms of thermal equilibrium physics.

Note that the equivalence exists on formal grounds only. There is no evident physical correspondence between the stochastic layer-by-layer growth process on the one hand and the thermodynamic equilibrium of the two-layer system on the other. Remember that the equivalence described here applies to the *asymptotic* statistics of the GM ($z\rightarrow\infty$).

The theorem presented in this section is similar to that given in Ref. [8], where a model for growth of binary alloys is considered, and where the asymptotic layer statistics was proved to be equivalent to the thermal equilibrium statistics of a two-layer system. Unlike our theorem, the interaction between the two layers of their equilibrium system is exactly the same as that assumed in their growth process. The complication in our case goes back to a lack of symmetry: their interaction governing the growth process is symmetric with respect to an exchange of the two layers; ours is not.

### B. The asymptotic distribution of layer pairs

The correspondence between the growth process GM and the two-layer system LL goes even beyond the one-layer statistics. In the present section we shall prove that the distribution of layer *pairs* is the same: $\Pi_{\sigma'\sigma}^{\mathrm{GM}}=\Pi_{\sigma'\sigma}^{\mathrm{LL}}$. Here, the first symbol refers to the growth process (GM; $z\rightarrow\infty$) and denotes the probability of finding two consecutive layers in given states $\sigma',\sigma$; the second symbol denotes the probability of the two-layer system LL to have its first and second layer in states $\sigma'$ and $\sigma$, respectively. In other words, the joint statistics of two consecutive layers of the growth process may be viewed as a canonical distribution of an appropriate two-layer system.

With the formulas of the preceding sections, the proof is simple. From the assumptions of the growth model we have

$$\Pi_{\sigma'\sigma}^{\mathrm{GM}} = \pi_{\sigma'}P_{\sigma'\sigma}. \tag{28}$$

Inserting $\pi_{\sigma'}$ from Eq. (20) and $P_{\sigma'\sigma}$ from Eq. (15), we obtain

$$\Pi_{\sigma'\sigma}^{\mathrm{GM}} = ce^{N_{\sigma'}^{+}D+N_{\sigma'}^{-}A}\Gamma_{\sigma'}\Lambda_{\sigma'\sigma}\Gamma_{\sigma}. \tag{29}$$

On the other hand, the probability $\Pi_{\sigma'\sigma}^{\mathrm{LL}}$ of a state $(\sigma',\sigma)$ of the two-layer system is proportional to $K_{\sigma'\sigma}$ and the explicit expression (22) for $K_{\sigma'\sigma}$ matches the expression given for $\Pi_{\sigma'\sigma}^{\mathrm{GM}}$ in Eq. (29). This completes the proof.

## VI. TWO-LAYER SYSTEM: BETHE-PEIERLS DESCRIPTION

In the preceding section we have shown that the asymptotic one- and two-layer statistics of the growth model is equivalent to the canonical distribution of an appropriate two-layer system. Thus, the asymptotic statistics of the growing system is reduced to a thermal equilibrium problem, which can be approached by many proven approximation methods. In the present section, we follow the guidelines of the Bethe method.

The application of Bethe's method to the antiferromagnetic phase transition of the Ising model with the inclusion of an external magnetic field was treated a long time ago [14,15]. In the present situation, this treatment has to be extended to two layers, $L'$ and $L$, and must include also the Ising interaction between the layers.

Within layer $L'$ we consider a site $(x,y)$ and its four nearest neighbors, polarities being denoted by $s'_0$ and $s'_k$ ($k=1,\ldots,4$). The polarities of the corresponding sites of layer $L$ are denoted by $s_0$ and $s_k$ ($k=1,\ldots,4$). In writing down the partition sum of this subsystem consisting of ten molecules, the internal pair interactions and the interaction with the field $B$ can be taken care of exactly, whereas the influence of the environment onto the $2\times4$ peripheral polarizations is approximated by mean fields $V^{(g)}$. Note that $V^{(g)}$ may depend on which sublattice $g$ ($g=1,2$; $x+y$ odd or even) the central sites of our subsystem belong to. $V^{(1)}$ and $V^{(2)}$ will then be determined from requirements of consistency (see below).

The partition sum of our subsystem reads

$$Z^{(g)}=\sum_{\alpha}\ \exp(-u^{(g)}_\alpha), \qquad (30)$$

the sum extending over all 1024 states $\alpha=\{s'_0,\ldots,s'_4,s_0,\ldots,s_4\}$. The symbol $u^{(g)}_\alpha$ collects all interactions mentioned above:

$$u^{(g)}_\alpha=\frac{Q_\parallel}{2}s'_0 s_0+B(s'_0+s_0)+\sum_{k=1}^{4}\left[\frac{Q_\parallel}{2}s'_k s_k+B(s'_k+s_k)\right.$$

$$\left.+\frac{Q_\perp}{2}(s'_0 s'_k+s_0 s_k)+V^{(g)}(s'_k+s_k)\right]. \qquad (31)$$

The explicit expression for $Z^{(g)}$ can be simplified, since all four peripheral pairs ($k=1,\ldots,4$) give rise to the same factor $\Omega^{(g)}(s'_0,s_0)$,

$$Z^{(g)}=\sum_{s'_0,s_0} Z^{(g)}(s'_0,s_0), \qquad (32)$$

$$Z^{(g)}(s'_0,s_0)=[\Omega^{(g)}(s'_0,s_0)]^4\times\exp\left[-\frac{Q_\parallel}{2}s'_0 s_0-B(s'_0+s_0)\right], \qquad (33)$$

$$\Omega^{(g)}(s'_0,s_0)=\sum_{s',s}\ \exp\left[-\frac{Q_\parallel}{2}s's-B(s'+s)\right.$$

$$\left.-\frac{Q_\perp}{2}(s'_0 s'+s_0 s)-V^{(g)}(s'+s)\right].$$

The expectation value of the sum of the two central polarizations is

$$\langle s'_0+s_0\rangle^{(g)}=\frac{2}{Z^{(g)}}[Z^{(g)}(+,+)-Z^{(g)}(-,-)], \qquad (34)$$

whereas the expectation value of the sum of a pair of peripheral polarizations can be obtained by differentiating with respect to $V^{(g)}$,

$$\langle s'_k+s_k\rangle^{(g)}=-\frac{1}{4}\frac{1}{Z^{(g)}}\frac{\partial}{\partial V^{(g)}}Z^{(g)}. \qquad (35)$$

Finally, the consistency requirements can be written down (central spins of one sublattice are the peripheral spins of the other sublattice):

$$\langle s'_0+s_0\rangle^{(1)}=\langle s'_k+s_k\rangle^{(2)}, \qquad (36)$$

$$\langle s'_0+s_0\rangle^{(2)}=\langle s'_k+s_k\rangle^{(1)}. \qquad (37)$$

For a given set of couplings ($A$, $D$, $Q_\perp$), Eqs. (36) and (37) constitute the equations for the determination of $V^{(1)}$ and $V^{(2)}$. They are polynomial equations of high degree, which can be solved numerically (we have used the MATHEMATICA system [16] for the numerical treatment). The probabilites of the different states of the subsystem are then known (being proportional to their contribution to the partition sum), as well as other characteristics of the system, such as, for example, the covariance $\langle s'_0 s'_k\rangle$ of adjacent polarizations.

Figure 4(b) displays the dependence of the sublattice polarizations and of the mean polarization on the coupling $Q_\perp$ for the parameter set $A=2.0$, $D=0.8$ as obtained from the Bethe approximation. The AFO-phase transition occurs at $Q_\perp^{(\mathrm{crit})}\approx0.44$, to be compared with a value of about 0.53 obtained from simulations of the two-layer system with the same parameters and with side length $d=50$. This is some improvement over the mean field approximation, which yields a critical value of about 0.33 in the same situation. In both approximations, the difference of sublattice polarizations rises with a critical exponent of $1/2$.

The parameter range in ($A$, $D$, $Q_\perp$) space allowing for an AFO transition can be derived from Eqs. (36) and (37). The numerical results are displayed in Fig. 5, where the critical value $Q_\perp^{(\mathrm{crit})}$ is given as a function of $A$ and $D$. We restrict ourselves to a sketch of the derivation. For given ($A,D,Q_\perp$), Eqs. (36) and (37) each define a curve, $C^{(1)}$ and $C^{(2)}$, in the plane of the variables $V^{(1)}$, $V^{(2)}$. Due to the symmetry between the two sublattices, the two curves are symmetric with respect to the diagonal $V^{(1)}=V^{(2)}$. The intersections of the two curves are the solutions of Eqs. (36) and (37). As expected, for low values of $Q_\perp$ there is only the symmetric solution, whereas there are three solutions for sufficiently
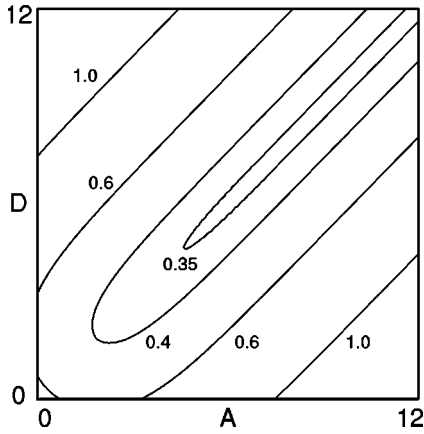
FIG. 5. Phase diagram in the quadrant $A>0$, $D>0$: critical value $Q_\perp^{(\mathrm{crit})}$ of $Q$ as a function of $A$, $D$. Bethe approximation. Axes: $A$, $D$. Parameter: $Q_\perp^{(\mathrm{crit})}$.

large values of $Q_\perp$. The limiting case, corresponding to the phase transition, is characterized by the curves $C^{(1)}$ and $C^{(2)}$ intersecting the diagonal with a slope of $-1$. The slope of the curves (especially at $V^{(1)}=V^{(2)}$) can be obtained by differentiating Eqs. (36) and (37) with respect to $V^{(1)}$, $V^{(2)}$, from where the critical condition can be formulated. The results displayed in Fig. 5 were obtained numerically.

Both in the mean field approximation as well as in the Bethe approximation the mean polarization exhibits a kink when tracked as a function of $Q_\perp$ [Figs. 4(a) and 4(b)]. Likewise, a kink is expected in the dependence of the mean polarization on the temperature at fixed coupling energies $\Delta E_A$, $\Delta E_D$, $\Delta E_\perp$. Figure 6 displays the polarization for the couplings $A=2.0T_0/T$, $D=0.8T_0/T$, $Q_\perp=0.54T_0/T$ as a function of $T/T_0$, where $T$ is the temperature and $T_0$ is an arbitrary reference temperature (dimensionless notation for fixed coupling energies). The kink corresponds to the phase transition in the Bethe approximation. In addition, Fig. 6 displays the results of our Monte Carlo simulations; again, no kink is observed here. The critical point obtained from simulations is indicated by the dotted curves (begining of the sublattice branches; they are bent towards lower temperatures).
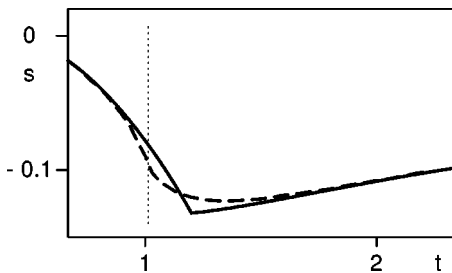


FIG. 6. Layer polarization $s$ in the large-$z$ limit. $A=2.0T_0/T$, $D=0.8T_0/T$, $Q_\perp=0.54T_0/T$. Abscissa: $t=T/T_0$ ($T$, temperature; $T_0$, arbitrary reference temperature). Ordinate: average layer polarization $s$. Solid line: mean polarization (Bethe approximation). Broken line: mean polarization (simulation results). Dotted line: sublattice polarizations as estimated from simulations (curves bent to the left).

In both approximations treated here, the phase transition is not destroyed by the external field influencing the two-layer system. This is in accordance with the behavior of the two-dimensional Ising model, where the antiferromagnetic phase transition survives an external magnetic field provided it is below a critical value [17–20].

To summarize the main results of the present paper, we have analyzed a specific growth process characterized by an infinite sequence of thermal equilibrium adherence of new layers onto previously formed layers, which then are assumed to be frozen. The thermal equilibrium of the adhered layer is governed by longitudinal and transverse Ising-type couplings. As stated previously [4], this sequence of processes leads to the formation of bulk polarization. In the present paper we are mainly concerned with the fact that this sequence of processes leads asymptotically to a stationary two-layer statistics. Depending on the signs and magnitudes of the coupling constants, the single layer may be FO or AFO ordered, and from one layer to the next local, polarizations may tend to reproduce or flip. Our main theoretical results concern the equivalence of the asymptotic two-layer statistics of this growth process with the canonical distribution of an appropriate two-layer system with Ising-like nearest neighbor couplings. We have made use of this equivalence, in that we have analyzed the asymptotic two-layer statistics by means of a Bethe-Peierls treatment. We have written simulation programs for the growth process and for the canonical distribution of the two-layer equivalent system. The present analysis explains the phenomena of growth-induced polarity formation as observed in real materials [5] and is intended to provide a systematic theoretical elaboration of possible phenomena for any signs of the couplings involved.

### APPENDIX: ISOLATED CHAIN

For an isolated chain, the states $\sigma$ of a layer reduce to the two polarizations $s=\pm 1$ of one molecule. The distribution $\pi$ of the polarization in the long chain limit ($z\to\infty$) is determined by the condition

$$\sum_{s'} \pi_{s'} P_{s's} = \pi_s, s=\pm 1, \tag{A1}$$

with the transition probabilities $P_{s's}$

$$P_{++}=1/(1+e^{-D}), \quad P_{+-}=e^{-D}/(1+e^{-D}),$$

$$P_{-+}=e^{-A}/(1+e^{-A}), \quad P_{--}=1/(1+e^{-A}). \tag{A2}$$

The normalized solution reads

$$\pi_+=(1+e^D)/(2+e^A+e^D), \tag{A3}$$

$$\pi_-=(1+e^A)/(2+e^A+e^D). \tag{A4}$$

[1] J. Hulliger, P. Rogin, A. Quintel, P. Rechsteiner, O. König, and M. Wübbenhorst, Adv. Mater. **9**, 677 (1997).

[2] A. Quintel, J. Hulliger, and M. Wübbenhorst, J. Phys. Chem. B **102**, 4277 (1998).

[3] P. Rechsteiner, J. Hulliger, and M. Flörsheimer, Chem. Mater. **12**, 3296 (2000).

[4] J. Hulliger, S.W. Roth, A. Quintel, and H. Bebie, J. Solid State Chem. **152**, 49 (2000).

[5] J. Hulliger, H. Bebie, S. Kluge, and A. Quintel, Chem. Mater. **14**, 1523 (2002).

[6] J. Hulliger, Z. Kristallogr. **214**, 9 (1999).

[7] S. Kluge, F. Budde, I. Dohnke, P. Rechsteiner, and J. Hulliger, Appl. Phys. Lett. **81**, 247 (2002).

[8] B. Drossel and M. Kardar, Phys. Rev. E **55**, 5026 (1996).

[9] L. Turi and J.J. Dannenberg, J. Phys. Chem. **97**, 12197 (1993).

[10] J. Hulliger and P.J. Langley, Chem. Commun. (Cambridge), 2557 (1998).

[11] J. Hulliger, M. Alaga-Bogdanović, and H. Bebie, J. Phys. Chem. B **105**, 8504 (2001).

[12] W.H. Press, B.P. Flannery, S.A. Teukolsky, and W.T. Vetterling, *Numerical Recipes* (Cambridge University Press, Cambridge, 1989), Sec. 7.1, generator RAN0.

[13] S. Eugster, Master's thesis, University of Berne, 2000.

[14] U. Firgau, Ann. Phys. (Leipzig) **40**, 295 (1941).

[15] P.W. Kasteleijn, Physica (Amsterdam) **12**, 387 (1956).

[16] S. Wolfram, *The Mathematica Book*, 4th ed. (Wolfram Media Cambridge, 1999).

[17] M.N. Barber, in *Phase Transitions and Critical Phenomena*, edited by C. Domb and J.L. Lebowitz (Academic Press, London, 1983), Vol. 8, p. 230 (see also original papers cited therein).

[18] E. Müller-Hartmann and J. Zittartz, Z. Phys. B **27**, 261 (1977).

[19] L. Sneddon, J. Phys. C **12**, 3051 (1979).

[20] S.-P. Hong, C.-S. Kim, S.-S. Lee, and S.-H.S. Salk, Phys. Rev. B **60**, 9252 (1999).